Development of Digital MRI Consoles Using General-Purpose Digital Instruments and Microcontroller Boards

Makoto Tsuda, Daiki Tamada, Yasuhiko Terada & Katsumi Kose

Applied Magnetic Resonance

ISSN 0937-9347

Appl Magn Reson
DOI 10.1007/s00723-016-0806-4

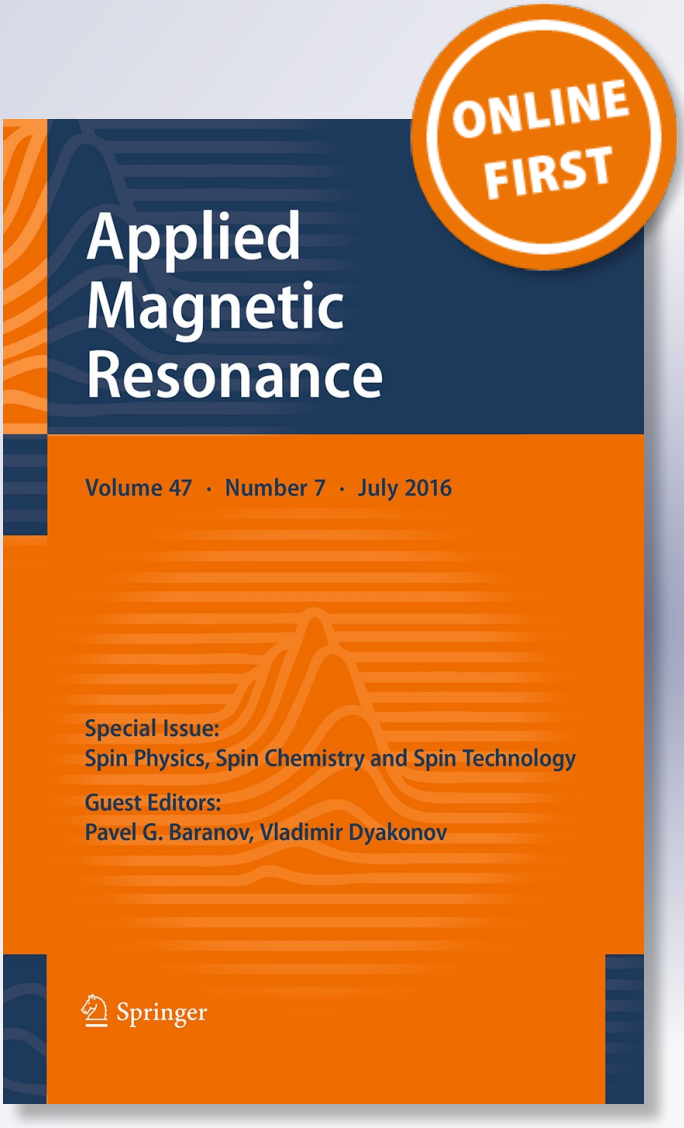

Springer

Appl Magn Reson
DOI 10.1007/s00723-016-0806-4

Applied
Magnetic Resonance

Development of Digital MRI Consoles Using General-Purpose Digital Instruments and Microcontroller Boards

Makoto Tsuda[1] · Daiki Tamada[1] · Yasuhiko Terada[1] · Katsumi Kose[1]

Received: 31 March 2016

Abstract We developed two digital magnetic resonance imaging (MRI) consoles using general-purpose digital instruments and microcontroller boards. The first console consisted of a digital oscilloscope (8-bit resolution, 250-MHz sampling frequency), an arbitrary waveform generator (14-bit resolution, 100-MHz sampling frequency), and three 32-bit microcontroller boards. The second console consisted of a digital oscilloscope (16-bit resolution, 1-GHz sampling frequency) with a built-in waveform generator (14-bit resolution, 200-MHz sampling frequency) and three 32-bit microcontroller boards. MRI experiments were performed using a 1.0-T and 90-mm gap yokeless permanent magnet to evaluate the MRI consoles. Three-dimensional spin-echo and gradient-echo images were successfully acquired using the first and second MRI consoles using an undersampling technique and RF phase correction. We concluded that the digital MRI consoles could be built using general-purpose digital instruments and microcontroller boards at a reduced cost and within a short development time.

1 Introduction

Since the proposal of magnetic resonance imaging (MRI) using a continuous wave nuclear magnetic resonance (NMR) spectrometer [1], there have been continuous progress in both the hardware and software of such systems. The progress in hardware includes large-bore superconducting magnets with high and homogeneous fields, fast and intense magnetic field gradient-coil systems, multiple RF coils with high sensitivity for parallel imaging, and sophisticated digital MRI console systems. The initial trials for digital MRI consoles were published late 1980s [2–4]. After the

✉ Katsumi Kose
kose@bk.tsukuba.ac.jp

[1] Institute of Applied Physics, University of Tsukuba, Tsukuba 305-8573, Japan

Published online: 30 June 2016

initial trials, the major manufacturers of human MRI systems have launched digital MRI console systems in the 1990s and 2000s. However, the published literature was very limited [5]. In contrast, academic institutions have published various approaches to digital MRI consoles since 1990s [6–14]. However, because, in such systems, they used sophisticated hardware, such as field programmable gate arrays (FPGAs) and digital signal processors (DSPs), the development costs were high, and the development time was very long.

In recent years, however, rapid developments in digital electronics have drastically extended the performance of such systems and have reduced their cost. For example, a dual channel digital oscilloscope with 15-bit resolution and 125-MHz sampling speed can now be purchased for ~$1000. Such digital instruments can change the approach to digital MRI consoles.

In this study, we developed two digital MRI consoles using digital oscilloscopes, arbitrary waveform generators, and microcontroller boards to demonstrate the validity of the above approach. The performance of the digital MRI consoles was tested using a 1.0-T permanent magnet MRI system, which demonstrated the usefulness of our approach.

2 Hardware

2.1 Digital MRI Console with an Independent Waveform Generator

An overview and a block diagram of the first (type A) digital MRI console are shown in Fig. 1. Type A console consisted of a digital oscilloscope (PicoScope 3205B, Pico Technology, St Neots, UK), an arbitrary waveform generator (AWG-100, ELMOS, Osaka, Japan), three 32-bit microcontroller boards (Arduino Due, Smart Project, Torino, Italy), and a laptop PC (Let's note CF-S9, Panasonic, Osaka, Japan).

The digital oscilloscope has two-channel inputs with 8-bit vertical resolution, 250-MHz maximum speed for two-channel simultaneous sampling, and 32-M word memory for each channel. The waveform generator has 50 Ohm and ±1.0 V maximum analog output with 14-bit resolution, 8-bit digital output, 100-MHz maximum sampling speed, and 1-M word wave memory for both analog and digital outputs. The microcontroller board has a 32-bit ARM Cortex-M3 RISC processor with 84-MHz clock frequency, 96-kB SRAM, 54 digital input/output (I/O) pins, and two 12-bit digital-to-analog (DA) converter outputs.

All the digital instruments and microcontroller boards were connected to the PC via universal serial bus (USB) cables (Fig. 1) and were controlled by the PC running under the Windows 7 operating system (Microsoft, Redmond, WA, USA).

2.2 Digital MRI Console Without an Independent Waveform Generator

An overview and a block diagram of the second (type B) digital MRI console are shown in Fig. 2. Type B console consisted of a digital oscilloscope (PicoScope 5242B, Pico Technology), three 32-bit microcontroller boards (Arduino Due), and a

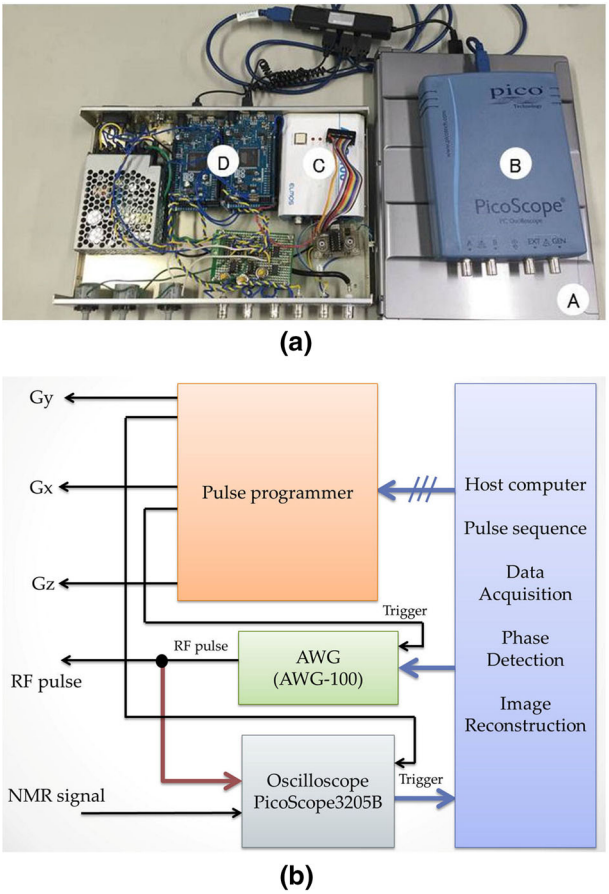

Fig. 1 **a** Overview and **b** block diagram of type A digital MRI console. Type A console consists of a laptop PC (*A*), a digital oscilloscope (*B*), an arbitrary waveform generator (*C*), and three 32-bit microcontroller boards (*D*)

laptop PC (15P5200-i5-QZB, Iiyama, Tokyo, Japan). The digital oscilloscope had two-channel inputs with 16-bit maximum vertical resolution and 1-GHz maximum speed, and a built-in arbitrary waveform generator output with 200-MHz sampling frequency. Because the digital oscilloscope included the waveform generator function, an independent waveform generator was not needed.

2.3 Pulse Programmer Using Microcontrollers

A block diagram of the pulse programmer used for the digital MRI consoles is shown in Fig. 3. The pulse programmer consisted of three microcontroller boards, one of which operated as a "master" pulse generator and two of which operated as "slave" pulse generators triggered by the master pulse generator. The slave

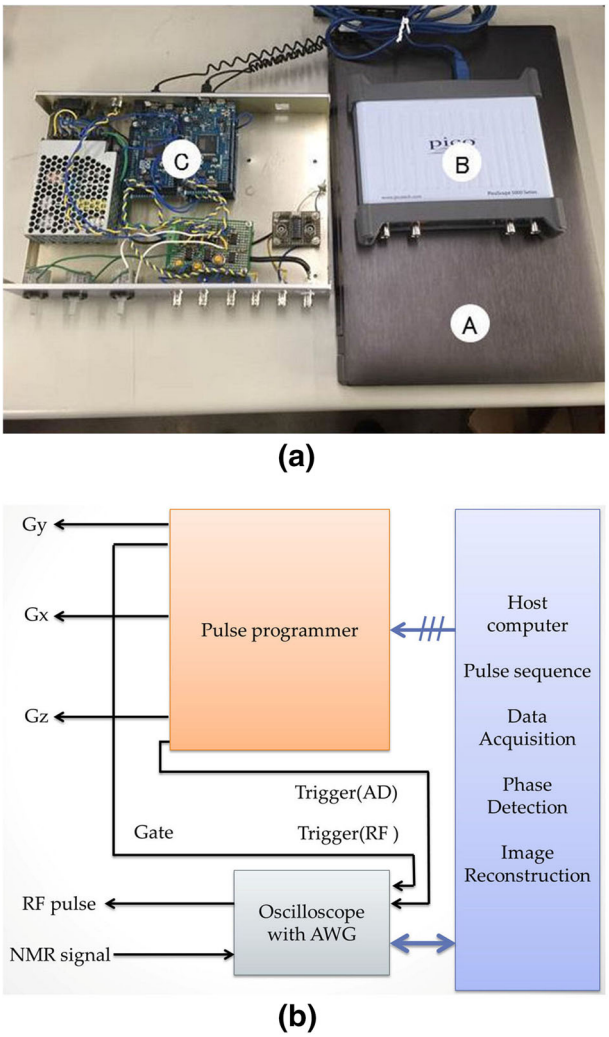

Fig. 2 **a** Overview and **b** block diagram of type B digital MRI console. Type B console consists of a laptop PC (*A*), a digital oscilloscope including an arbitrary waveform generator (*B*), and three 32-bit microcontroller boards (*C*)

microcontroller boards were connected to the master microcontroller board via a digital I/O to synchronize the output timing. The waveforms for the gradient coils Gx, Gy, and Gz were the outputs from the DA converters of the microcontroller boards. These DA outputs were connected to the inputs of the gradient drivers of the 1.0-T MRI system described later. The sampling trigger signal for the digital oscilloscopes was the output from the master microcontroller, and the trigger signal for the arbitrary waveform generator was the output from the slave microcontroller.

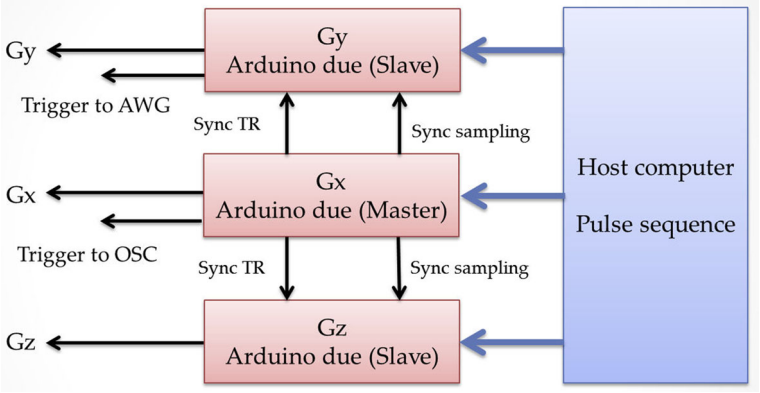

Fig. 3 Block diagram of the pulse programmer using three microcontroller boards. The master microcontroller generates the exact timing for the repetition time (TR) and for pulse programmer events that are synchronized with the slave microcontrollers using digital input/output pins

2.4 1.0-T Permanent Magnet MRI System

The MRI consoles described in the previous subsections were evaluated using a permanent magnet MRI system originally developed for mouse imaging [15]. The MRI system consisted of a 1.0-T field strength and 90-mm gap yokeless permanent magnet (NEOMAX Engineering, Takasaki, Japan), a home-built 72-mm gap planar gradient-coil set, a home-built RF probe (six-turn solenoid coil, 32 mm inner diameter), and an analog MRI console (MRTechnology, Tsukuba, Japan). The Larmor frequency was 43.85 MHz, and a bandpass filter (−3 dB passband: 34–54 MHz) was inserted at the front-end of the MRI receivers of the digital MRI consoles. The bandpass filter was made by connecting the low-pass and high-pass filters with 50-MHz cutoff frequencies (Model BLP-50 and Model BHP-50, Mini-Circuit, Brooklyn, NY, USA) in series.

3 Software

The block diagram of the MRI control software programs developed for type A console is shown in Fig. 4. The programs were developed using Qt 5.3.0 and C++ running under the Windows 7 operating system. A typical three-dimensional (3D) spin-echo imaging pulse sequence file is shown in Fig. 5. The first five lines of the sequence file show numbers of the phase-encoding steps (S1 and S2), increments of the phase encoding amplitudes (N1 and N2), and the repetition time (TR) of the pulse sequence in milliseconds. The following lines represent timings of events written by second, millisecond, and microsecond separated by periods, names of events written by two capital letters, and (gradient) amplitudes or kinds for the events.

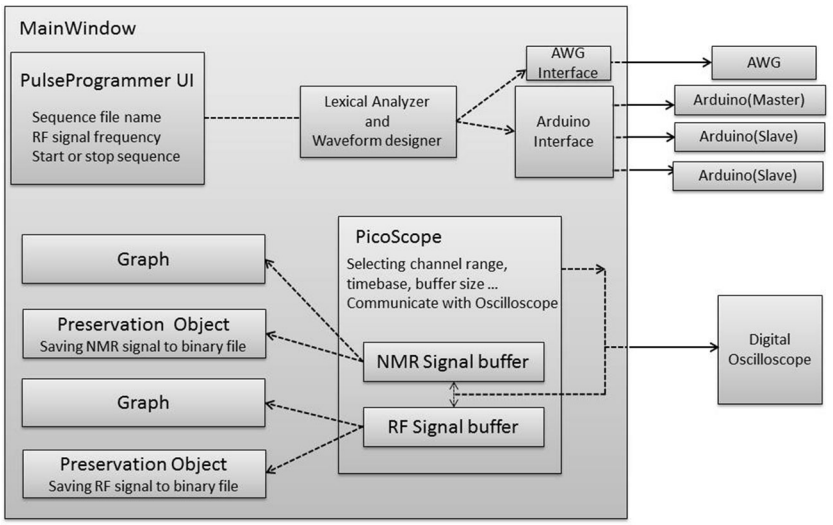

Fig. 4 Block diagram of the digital MRI control program for type A console

Fig. 5 Sequence file for the spin-echo 3D imaging sequence. The initial five lines show numbers of the phase encoding steps (*S1* and *S2*), increments of phase-encoding gradient amplitudes (*N1* and *N2*), and repetition time (*TR*). The following lines represent timings of events, names of events, and (gradient) amplitudes or kinds for the events

```
;S1=16
;S2=16
;N1=128
;N2=16
;TR=1000

00.010.000 RF 0002

00.010.220 GY 0E2E
00.014.580 GY 0800

00.015.440 AD 0FFF
00.015.940 RF 0003

00.016.160 GX 1FFF
00.016.260 GZ 2FFF

00.017.480 GY 0E2E
00.018.060 GX 0800
00.018.169 GZ 0800
00.027.120 GY 0800
```

First, the program shown in Fig. 4 reads the sequence file, interprets it line by line using the rule described above, constructs waveforms for the gradient-coil currents, and downloads the target programs developed using the Arduino integrated

development environment (IDE), gradient and RF waveforms, and the sequence data to the microcontrollers and the arbitrary waveform generator. The master microcontroller generates an exact timing for TR and exact timings for the events every 20 μs using timer interrupt operations according to the downloaded programs. The timings of TR and the event are sent to the slave microcontrollers via the I/O pins (see Fig. 3). In this way, the outputs of the RF pulses, data-acquisition, and gradient waveforms (Gx, Gy, and Gz) were synchronized according to the exact timing of the time base of the master microcontroller.

The acquired MRI signal and RF source signal data are transferred from the digital oscilloscopes to the PC via the USB 2.0 interface every TR of the pulse sequences. Because the time required for data-transfer limited the minimum TR, we used the undersampling technique to reduce the data size.

4 Experiments

4.1 Phantoms and Pulse Sequences

A water phantom consisting of glass capillaries (outer diameter, o.d. = 2.5 mm, inner diameter, i.d. = 2.0 mm) stored in a test tube (o.d. = 30 mm, i.d. = 28 mm) filled with $CuSO_4$ water solution and a chemically fixed mouse were used for imaging experiments using type A console. A water phantom consisting of acrylic pipes (o.d. = 5.0 mm, i.d. = 3.0 mm) stored in a glass test tube (o.d. = 20 mm, i.d. = 17 mm) filled with $CuSO_4$ water solution was used for imaging experiments using type B console.

For type A console, two-dimensional (2D) and 3D spin-echo imaging sequences were used. The TR and the spin-echo time (TE) for the sequences were 400 and 11.9 ms, respectively. The image matrix and the field of view (FOV) were 256 × 256 and 35 mm × 35 mm for the 2D sequence and 256 × 128 × 16 and 77.3 mm × 33.4 mm × 19.2 mm for the 3D sequence. For type B console, a 3D gradient-echo imaging sequence with TR = 200 ms, TE = 11.1 ms, image matrix = 256 × 256 × 16, FOV = 38.5 mm × 34.5 mm × 30.4 mm, and flip angle = 90° was used.

4.2 Data Sampling

The MRI signal was sampled at about 6.944444-MHz sampling frequency (with 144-ns sampling interval) for 14.4 ms (100,000 data points). For type A console, the MRI signal was sampled using the first channel, and the source RF signal of the 180° pulse generated by the arbitrary waveform generator was synchronously sampled using the second channel for the phase correction. For type B console, the 90° pulse through the preamplifier was sampled before the gradient-echo signal using the identical channel. The phase of the 90° RF pulse was used for the phase correction of the MRI signal.

5 Results

The MRI signal and the source of the RF pulse synchronously sampled using the oscilloscope are shown in Fig. 6. 30,000 data points (4.32 ms) selected from the sampled MRI signal data (100,000 points) were transformed using Fourier transform to obtain the frequency spectra of the MRI signal. The frequency of the spin-echo signals was centered at around 2.183 MHz, because the 43.85-MHz Larmor frequency of the MRI signal was converted down to $43.85 - (3.472222 \times 12)$ MHz. 256 complex (real and imaginary) points (59-kHz bandwidth) centered at 2.183 MHz were used for image reconstruction after the phase correction described below.

Because the phase of the RF pulse was initialized by the trigger pulse generated by the pulse programmer for every TR, it was determined by the base clock of the master microcontroller. On the other hand, the phase of the MRI signal was determined by the base clock of the oscilloscopes. Because the base clocks of the

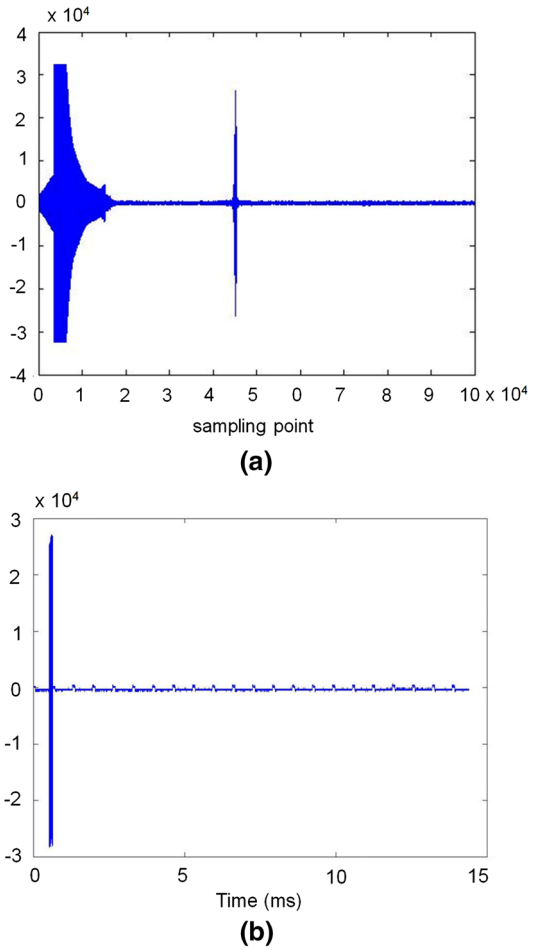

Fig. 6 **a** MRI signal and **b** RF source signal synchronously sampled at 144-ns time intervals. The MRI signal was sampled for 14.4 ms, and 100,000 points were acquired

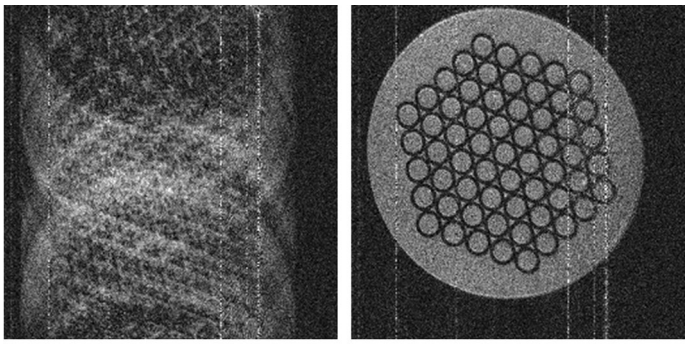

Fig. 7 2D MR images acquired using type A console **a** without and **b** with phase correction. TR = 400 ms, TE = 11.9 ms, slice thickness = 5 mm, FOV = 35 mm × 35 mm, matrix size = 256 × 256. The *vertical line* noise is external noise

master microcontroller and the oscilloscopes were independent, the relative phase between the RF pulse and the MRI signal varied for every TR. This resulted in the fact that the phase of the MRI signal changed from TR to TR. Therefore, the phase correction was indispensable to reconstruct MRI images from series of phase encoded MRI signals. For type A console, the phase correction was performed using the RF phase of the 180° pulse synchronously sampled using the second channel of the oscilloscope. For type B console, it was performed using the RF phase of the 90° degree (excitation) pulse sampled using the receiving channel identical to the MRI signal.

2D cross sections of the water phantom without and with the phase correction acquired using type A console are shown in Fig. 7a, b. The unpredictable signal phase caused by the independent time base used in the oscilloscope and the pulse programmer was precisely corrected. 16 horizontal cross sections selected from a 3D image data set of a chemically fixed mouse acquired with the 3D SE sequence using type A console are shown in Fig. 8, and a 2D cross section selected from a 3D image data set acquired with the 3D gradient-echo sequence using type B console is shown in Fig. 9. There was no phase ghosting in the gradient-echo image acquired using type B console.

6 Discussion

6.1 Phase Correction of the MRI Signal

If a single coherent time base is used for the transmitter and the receiver of a digital MRI system, the phase of the complex (real and imaginary) MRI signal is reproducible for any MRI pulse sequences. However, if the time base for the transmitter (or the pulse programmer) and that for the receiver are independent, such as in our case, the MRI signal phase changes from TR to TR. This unreproducible

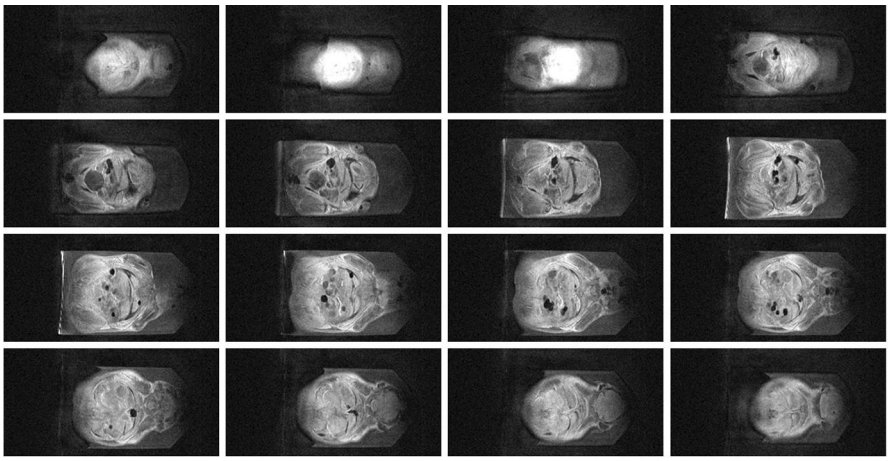

Fig. 8 Horizontal cross sections selected from a 3D image data set of a chemically fixed mouse acquired using type A console. TR = 400 ms, TE = 11.9 ms, FOV = 77.3 mm × 33.4 mm × 19.2 mm. Matrix size = 256 × 128 × 16

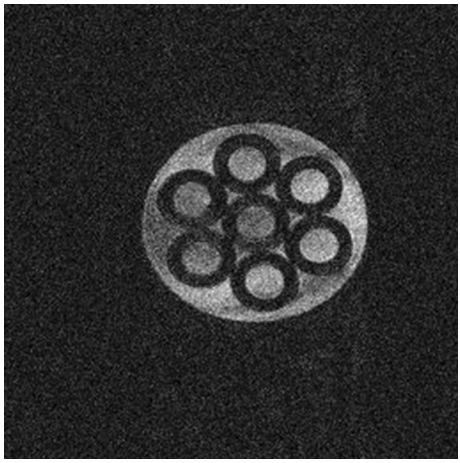

Fig. 9 2D cross section selected from a 3D image data set acquired with a 3D gradient-echo sequence using type B console

phase must be corrected to reconstruct MR images using the Fourier imaging method [16]. We corrected the MRI signal phase using following two different approaches.

The first approach was to sample the 180° pulse source signal synchronously with the MRI signal (Fig. 6). The phase correction using this approach worked very well (Fig. 7). The second approach was to use the 90° RF pulse signal measured before the gradient-echo signal. Although this approach worked well (Fig. 9), the dynamic range for MRI signal was limited, because the RF pulse signal was very large compared with the MRI signal. Therefore, type A is better than type B from the viewpoint of the signal dynamic range.

6.2 Undersampling

Because the maximum sampling speed of the digital oscilloscopes was 250 MHz and 1 GHz for type A and type B consoles, the undersampling technique was not needed to reproduce the MRI signal of 43.85 MHz. For type A console, to satisfy the Nyquist theorem, about 10-ns sampling interval is necessary and $1{,}440{,}000 \times 2 = 2{,}880{,}000$ points should be transferred from the oscilloscope to the PC for every TR. However, this data-transfer limited the minimum TR, which was essential to fast image acquisition. To solve this problem, we used the undersampling technique described in the above section.

Meanwhile, because the bandwidth of the MRI signal in the rotating frame is about 59 kHz in our imaging experiments, the 6.94444-MHz RF sampling was oversampling for the MRI signal. The oversampling ratio was about 120, corresponding to about 7-bit extension of the dynamic range of the analog-to-digital converter (ADC). Therefore, the use of 8-bit ADC in type A console is sufficient for MR image acquisition.

6.3 Comparison Between Type A and Type B Consoles

The arbitrary waveform generator used in type A console had 1-M word memory with 100-MHz maximum sampling speed. Therefore, coherent RF excitations for about 10 ms maximum can be used. The spin-echo (90°-TE/2-180° excitation) experiments could be performed using this RF pulse duration. In contrast, the arbitrary waveform generator built-in the digital oscilloscope used in type B console has only 32-K word memory with 200-MHz fixed sampling speed. Therefore, the duration of the RF pulse was limited to about 160 μs, which disabled use of spin-echo sequences. To summarize, type A console had a relatively complicated structure but was flexible for pulse sequence design, and type B console had a very simple structure, but the pulse sequence was limited to gradient-echo (single pulse) sequences.

7 Conclusion

We developed two digital MRI consoles using commercialized digital units and microcontroller boards and confirmed their performance using MRI experiments. The total costs for the consoles of types A and B excluding the PCs were about $1500 and $1200, respectively. Because the time required for the developments was about 1 year, we conclude that our approach is promising for the development of digital MRI consoles.

Acknowledgments We acknowledge Dr. Tomoyuki Haishi for the use of the 1.0-T permanent magnet MRI system and helpful discussions.

References

1. P. Lauterbur, Nature **242**, 190 (1973)
2. R. Proska, in *Proceedings of the 7th Annual meeting of the Society of Magnetic Resonance in Medicine*, San Francisco (1988), p. 266
3. G.N. Holland, D.M. Blakeley, J.R. Stauber, D. Flugan, K.S. Denison, in *Proceedings of the 8th Annual meeting of the Society of Magnetic Resonance in Medicine*, Amsterdam (1989), p. 182
4. R.S. Stormont, P.J.P. Noonan, N.J. Pelc, N.R. Hattes, M.D. Anas, R.H. Howarth, R. Glusick, in *Proceedings of the 8th Annual meeting of the Society of Magnetic Resonance in Medicine*, Amsterdam (1989), p. 962
5. J. Bollenbeck, M. Vester, R. Oppelt, H. Kroeckel, W. Schnell, Proc. Intl. Soc. Mag. Reson. Med. **13**, 860 (2005)
6. M. Kasal, J. Halámek, V. Husek, M. Villa, U. Ruffina, Proc. Cofrancesco Rev. Sci. Instrum. **65**, 1897 (1994)
7. K. Raoof, A. Asfour, J.M. Fournier, IEEE Instrumentation and Measurement Technology Conference, Anchorage, AK, USA (2002), p. 21
8. J. Bodurka, P.J. Ledden, P. van Gelderen, R. Chu, J.A. de Zwart, D. Morris, J.H. Duyn, Magn. Res. Med. **51**, 165–171 (2004)
9. P. Perez, A. Santos, Med. Eng. Phys. **26**, 523 (2004)
10. S. Jie, X. Qin, L. Yang, L. Gengying, Rev. Sci. Instrum. **76**, 105101 (2005)
11. S. Hashimoto, K. Kose, T. Haishi, Rev. Sci. Instrum. **83**, 053702 (2012)
12. P.P. Stang, S.M. Conolly, J.M. Santos, J.M. Pauly, G.C. Scott, IEEE Trans. Med. Imaging **31**, 370 (2012)
13. W. Tang, H. Sun, W. Wang, Rev. Sci. Instrum. **83**, 104701 (2012)
14. X. Liang, S. Binghe, M. Yueping, Z. Ruyan, Rev. Sci. Instrum. **84**, 054702 (2013)
15. T. Shirai, T. Haishi, S. Utsuzawa, Y. Matsuda, K. Kose, Magn. Reson. Med. Sci. **4**, 137 (2005)
16. A. Kumar, D. Welti, R.R. Ernst, J. Magn. Reson. **18**, 69 (1975)